Intermetallics 112 (2019) 106541

Contents lists available at ScienceDirect

Intermetallics

journal homepage: www.elsevier.com/locate/intermet

Enhancement in thermoelectric performance of single step synthesized Mg doped Cu_2Se: An experimental and theoretical study

Ruchi Bhardwaj[a,b], Amrita Bhattacharya[c,***], Kriti Tyagi[a], Bhasker Gahtori[a,b,**], Nagendra Singh Chauhan[a,b], Avinash Vishwakarma[a,b], Kishor Kumar Johari[a,b], Sivaiah Bathula[a,b], Sushil Auluck[a], Ajay Dhar[a,b,*]

[a] CSIR-National Physical Laboratory, Dr. K.S. Krishnan Marg, New Delhi, 110012, India
[b] Academy of Scientific & Innovative Research (AcSIR), CSIR-NPL Campus, New Delhi, 110012, India
[c] Department of Metallurgical Engineering and Materials Science, IIT Bombay, Mumbai, 400076, India

ARTICLE INFO

Keywords:
Thermoelectric
Copper-selenide
Figure-of-merit
Density functional theory
Thermal conductivity
Electrical conductivity

ABSTRACT

Copper selenide (Cu_2Se) is a simple binary compound which exhibits very fascinating thermoelectric properties, due to which it has been widely studied till very recently. This work highlights that the doping in Cu_2Se only affect the electronic transport while the thermal transport is not significantly influenced due to the liquid like dynamics of the Cu ions in the lattice that results in significant thermal instabilities to an extent that the effect of doping is negligible. Our experiments show that an enhanced ZT ~1.6 at 860 K was achieved in Mg-doped Cu_2Se, synthesized employing a facile single-step reactive spark plasma sintering technique, which is both fast and scalable. The experimental results indicate that Mg-doping in Cu_2Se leads to a significant enhancement in its electrical conductivity, which is primarily responsible for the significant improvement in the ZT. However, the lattice thermal conductivity was found to remain relatively unchanged, irrespective of the Mg-doping concentration, which is also in agreement with our DFT calculations.

1. Introduction

The deployment of thermoelectric generators (TEG) [1], which are able to convert a temperature gradient into an electric voltage using the Seebeck effect, are being seriously considered as an alternative to other existing sources of green energy. The efficiency of a thermoelectric material is related to its figure-of-merit [2,3] $ZT = S^2 \sigma T/\kappa$, where S is the Seebeck coefficient, σ the electrical conductivity, T is absolute temperature and κ ($= \kappa_e + \kappa_L$) the thermal conductivity, which has contributions from both the electronic (κ_e) and phononic (κ_L) parts. It is apparent that in order to increase the thermoelectric efficiency, the ZT has to be enhanced, which is purely a material dependent property. However, ZT cannot be maximized by separately optimizing the individual thermal and electrical transport coefficients, since they subtly depend on each other [1,4]. Among the several strategies adopted thus far, doping has been reported to be the most facile and effective in enhancing the ZT of thermoelectric materials [5–7].

Binary Cu_2Se has drawn considerable attention in the recent years as a promising thermoelectric material due to its reportedly high thermoelectric performance [8–17]. Cu_2Se exists in two phases: a stable low-temperature α-phase that transforms to the high-temperature β-phase at ~140 °C. While the α-phase has not still been fully understood as different groups have reported different structure at room temperature. A tetragonal structure was reported by Borchert [18], while Stevels [19] and Jellinek proposed an orthorhombic structure, Murray and Heyding revised the structure to monoclinic [20]. Later, using electron diffraction, Vucik and group suggested another monoclinic structure [21]. Further, Gulay et al. has also reported the monoclinic phase at room temperature [22], which was also endorsed by Liu et al. [9] and Yu et al. [10]. On the other hand, the crystal structure of β-phase has been determined to be cubic that crystallizes in Fm-3m space group [9,10,12,22]. In the β-Cu_2Se structure, Se atoms form a fcc-framework, while the Cu^+ ions are highly mobile that exhibit a liquid-like behaviour with a reduced phonon mean free path [9,23,24], which results in a low lattice thermal conductivity. Bulk Cu_2Se is an intrinsically a *p*-type semiconductor and has been reported to exhibit a ZT ~1.5 at

* Corresponding author. CSIR-National Physical Laboratory, Dr. K.S. Krishnan Marg, New Delhi, 110012, India.
** Corresponding author. CSIR-National Physical Laboratory, Dr. K.S. Krishnan Marg, New Delhi, 110012, India.
*** Corresponding author.
E-mail addresses: b_amrita@iitb.ac.in (A. Bhattacharya), bhasker@nplindia.org (B. Gahtori), adhar@nplindia.org (A. Dhar).

https://doi.org/10.1016/j.intermet.2019.106541
Received 20 February 2019; Received in revised form 4 June 2019; Accepted 10 June 2019
Available online 27 June 2019

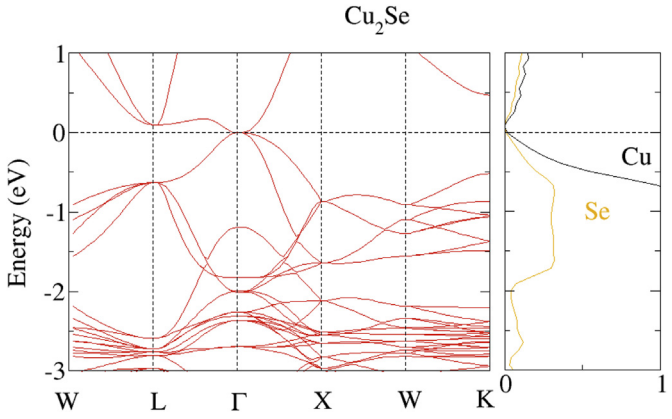

Fig. 1. Electronic band structure and Density of states of pristine cubic Cu_2Se calculated using GGA PBE.

1000 K [9], which was further enhanced to 1.9 on Te doping [16] and further shown to increase ~ 2.1 on nanostructuring [13]. Recently, a ZT value ~1.8 at 1000 K has been realized in pristine Cu_2Se synthesized employing a novel process of self-propagating high-temperature synthesis [15]. Also, Liu et al. [12] have reported a high ZT ~ 2.3 in Cu_2Se with I-doping, but this high thermoelectric performance was observed at its phase transition temperature. Zhong et al. have created highly aligned large lamellae in bulk $Cu_{1.94}Al_{0.02}Se$ using the direct-current hot pressing process, which although results in large peak ZT value but the obtained variation in ZT value indicated that the reproducibility of the ZT value among the as-prepared 50 samples is not good [25]. It has been established that despite its good thermoelectric performance [13], Cu_2Se is not a practical material for TEG applications owing to its serious issues related to Se evaporation and electro-migration of Cu ions [13,17,26], although recently it has also been reported that optimized doping and proper working conditions does improve its thermal stability [14,27,28]. Nevertheless, the premise of the current study is only to highlight strategies that can be adapted to select suitable dopant and enhance thermoelectric properties of Cu_2Se.

This work highlights the enhancement in the thermoelectric performance of Cu_2Se by employing Mg doping. An enhanced ZT ~1.6 at 860 K was realized in 1 at.% Mg-doped Cu_2Se, synthesized by employing a rapid single-step reactive spark plasma sintering technique. It was experimentally observed that although the electronic transport coefficients of Cu_2Se show a strong dependence on Mg-doping, the lattice thermal conductivity exhibits a rather weak dependence on the doping concentration. This has also been substantiated by our first-principles based DFT calculations, which show that the lattice thermal conductivity barely changes as a function of doping suggesting that liquid like behaviour of the Cu ions in Cu_2Se strongly dominates the phonon dynamics to an extent that doping-induced changes in the scattering lifetime of phonons are hardly noticeable.

2. Material and methods

$Cu_{2-x}Mg_xSe$ (x = 0 to 0.04) samples were synthesized by rapid one-step process of reactive sintering which lasted for a few minutes. The powders of the constituent elements were blended in a stoichiometric ratio and were subsequently consolidated and sintered under vacuum (~4 Pa) using spark plasma sintering (SPS Syntex, 725) at an optimized process parameters 60 MPa at 600 °C using graphite die and punches. Powder X Ray diffraction (Rigaku, 30 kV and 15 mA) was used for phase determination. Field Emission Scanning Electron Microscope (FESEM, *Zeiss, Supra 40VP) and* energy-dispersive x-ray spectroscopy were utilized to study the Morphology and elemental distribution of sintered samples. The polished sample disc of diameter 12.7 mm and thickness 2.5 mm was used for measurement of thermal diffusivity using the laser flash system (Linseis, LFA 1000). Electrical conductivity and Seebeck coefficient were measured simultaneously by using instrument Ulvac, ZEM 3 and the specific heat measurement was carried out by DSC (Netzsch, DSC 404 F3). Archimedes principle was employed to calculate the density of all the samples. Thermal conductivity was calculated as the product of thermal diffusivity, specific heat and the density. The accuracies for all the electrical and thermal transport measurements have been reported elsewhere [29]. In order to evaluate the carrier concentration and the mobility of charge carriers, the Hall measurements (HEMS, Nanomagnetics) were performed at room temperature.

2.1. Computational details

The DFT calculations [30,31] were performed using VASP [32], which is a plane wave based electronic structure code. We have used the generalized gradient approximation (GGA) as incorporated in the Purdue Burke Ernzerhof (PBE) exchange correlation functional [33] to perform all the theoretical calculations. In all the cases the atomic as well as geometric relaxations are executed using conjugate gradient method. All numerical settings are chosen so as to ensure a convergence in energy differences of less than 10^{-4} eV. The finite displacement method implemented in phonopy was used to calculate the phonon dispersion and the phonon DOS from the harmonic approximation [34,35]. The phonon scattering lifetimes and, therefore, the lattice thermal conductivity were directly evaluated from the third order force constants by using phono3py [36]. The DFT calculations were performed with the high temperature cubic anti-fluorite structure of β-Cu_2Se. In order to achieve the doping for the phonon calculations, we have substituted one of the 64 Cu atoms by Mg in 2 × 2 × 2 cell of β-Cu_2Se, which led to a doping of 1.5 at. %. Please note that for the

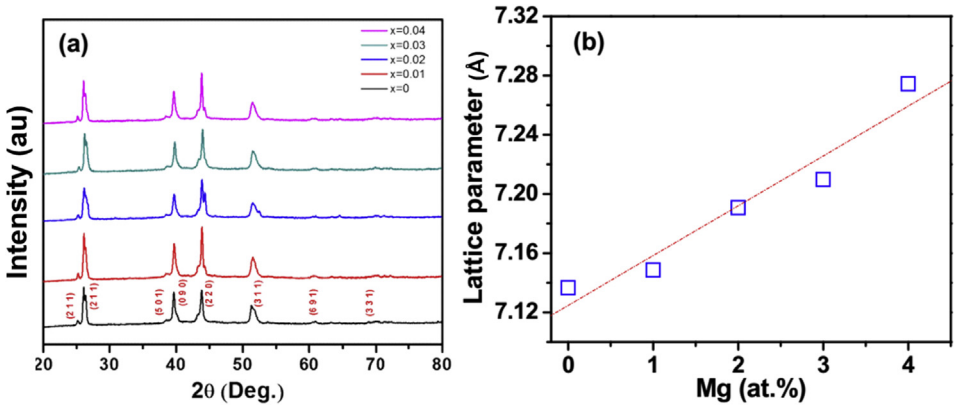

Fig. 2. (a) X-Ray Diffraction patterns of $Cu_{2-x}Mg_xSe$ samples and (b) Variation of lattice parameter of Cu_2Se with Mg-doping concentration.

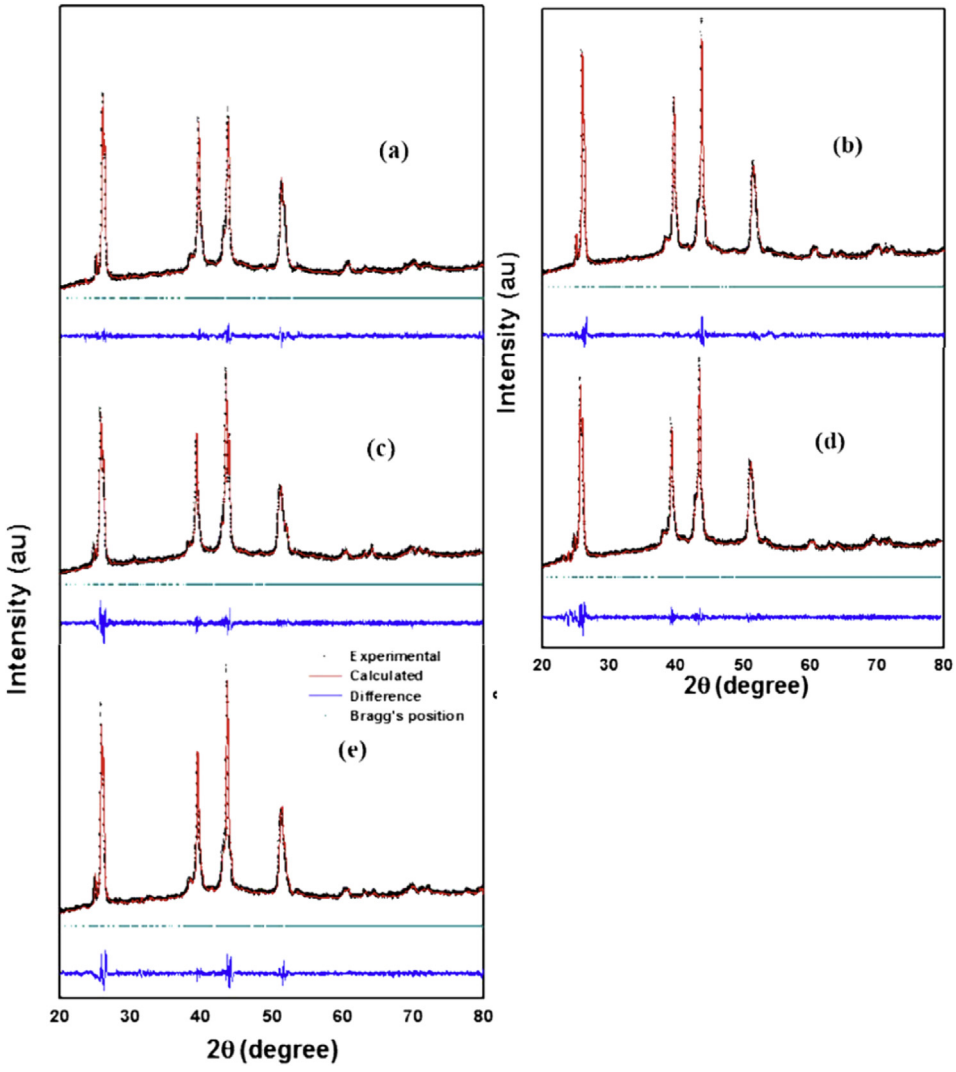

Fig. 3. Rietveld refined X-Ray diffraction patterns of $Cu_{2-x}Mg_xSe$ samples.

Table 1
Crystallographic Details from Rietveld Refinement of $Cu_{2-x}Mg_xSe$ samples.

Parameters	Cu_2Se	$Cu_{1\cdot99}Mg_{0\cdot01}Se$	$Cu_{1\cdot98}Mg_{0\cdot02}Se$	$Cu_{1\cdot97}Mg_{0\cdot03}Se$	$Cu_{1\cdot96}Mg_{0\cdot04}Se$
Phase	Monoclinic	Monoclinic	Monoclinic	Monoclinic	Monoclinic
a	7.13	7.14	7.19	7.20	7.27
b	12.43	12.46	12.51	12.56	12.45
c	27.41	27.48	27.58	27.77	27.45
$\alpha = \gamma$	90	90	90	90	90
β	93.90	94.10	94.03	94.12	94.56
χ^2	1.37	1.68	1.74	2.0	2.49
R_F	1.12	1.12	2.43	0.72	0.77
R_{Bragg}	0.88	0.90	1.39	0.69	0.79

phonon calculations we achieve the doping in such as a way that we can draw meaningful analogies with the experimental results.

3. Results and discussions

Our electronic band structure calculation based on GGA shows a semi-metallic band structure of β-Cu_2Se with the valence and conduction band meeting at the Γ [Fig. 1(a)], which is in agreement with the previous theoretical reports [37,38]. Please note that LDA/GGA based DFT calculations commonly underestimate the experimental electronic band gap. Particularly, in case of β-Cu_2Se opening the electronic band gap is found to be a very challenging problem under the framework of DFT (Fig. 1). For serving this purpose, we have also tested scissor operators and computationally more involved HSE06/Scissor operators, which have also failed to reproduce the experimental electronic band gap in this compound.

Fig. 2 (a), which shows the XRD patterns of the synthesized pristine and Mg-doped Cu_2Se, confirmed the formation of a single phase. To analyse the phase and the crystallographic structure of Cu_2Se and Mg doped Cu_2Se samples we have performed Rietveld refinement of XRD data by using Fullprof software. All the samples exhibit monoclinic crystal structure at room temperature and the space group is C 2/c (15)

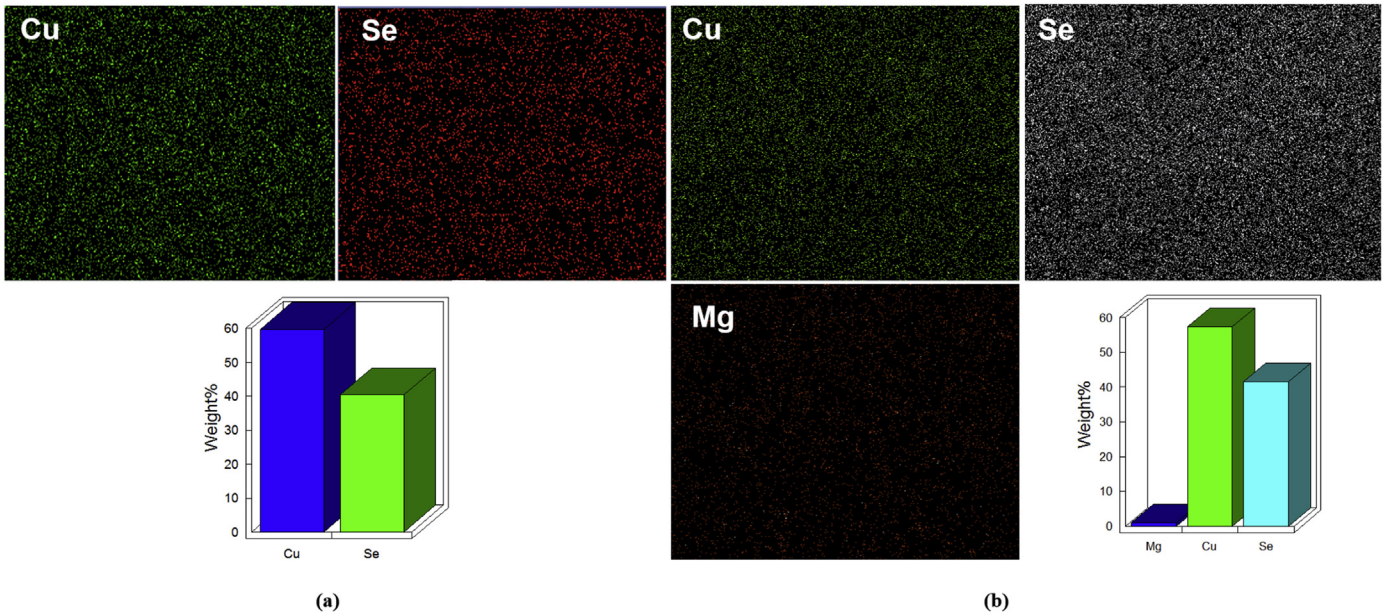

Fig. 4. Elemental distribution and weight% of constituent elements of (a) Cu_2Se, (b) Mg doped Cu_2Se.

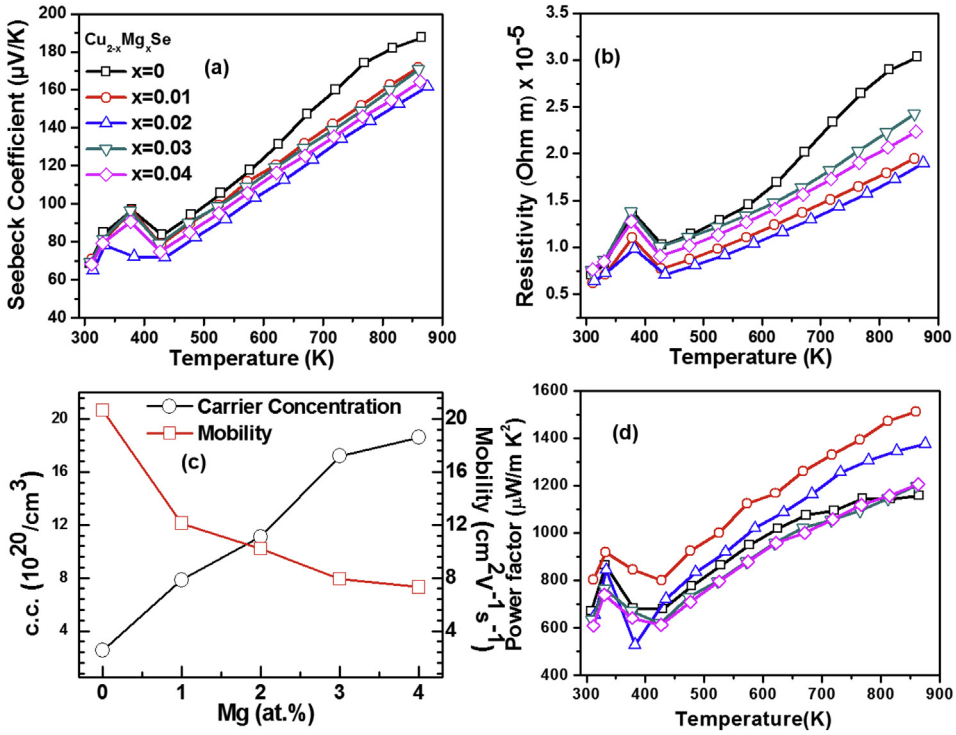

Fig. 5. Temperature dependence of the electrical transport properties of $Cu_{2-x}Mg_xSe$ (a) Seebeck coefficient, (b) electrical resistivity, (c) carrier concentration and charge mobility of $Cu_{2-x}Mg_xSe$ samples at room temperature with respect to doping concentration of Mg, (d) power factor.

and the crystal structure is in agreement with that reported by Gulay et al. [22]. The refined pattern as well as the parameters also confirms the purity of Cu_2Se single phase and express that the fitted and the experimental XRD patterns are in good agreement. The lattice parameter, evaluated from the XRD data, shows a linear increase with Mg-doping concentration (Fig. 2(b)), in accordance with the Vegard's law due to larger atomic radius of Mg (173 pm) as compared to Cu (128pm), thus suggesting the complete incorporation of the dopant in the Cu_2Se. The Rietveld refined XRD patterns are shown in Fig. 3 and the crystallographic parameters for all the synthesized samples are shown in Table 1. Fig. 4 shows the Energy-dispersive spectroscopy (EDS) results of the pristine and Mg-doped Cu_2Se samples, which indicates that the chemical composition of the synthesized samples is near to their original stoichiometry. It is also clear from the figure that elemental distribution is uniform throughout the sample ensuring the homogeneity of both the samples.

Temperature dependent electronic transport properties of the pristine and Mg-doped Cu_2Se samples are displayed in Fig. 5, which confirms a prominent phase transition from α to β phase of Cu_2Se at ~415 K [9,13]. The temperature dependence of the Seebeck coefficient for the pristine and Mg doped Cu_2Se samples is shown in Fig. 5(a) and its positive sign suggests that holes are the majority charge carriers

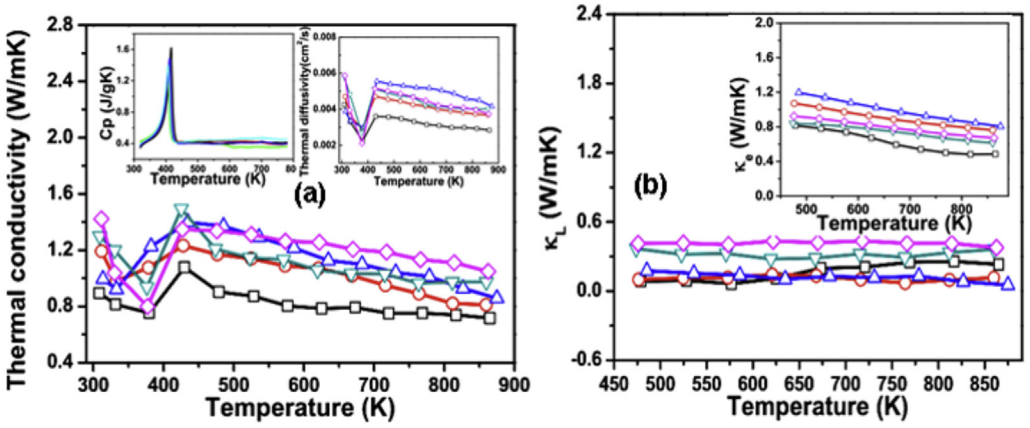

Fig. 6. Temperature dependence of the thermal properties of $Cu_{2-x}Mg_xSe$ (a) thermal conductivity (thermal diffusivity and C_P in inset) and (b) lattice thermal conductivity with electronic thermal conductivity (inset).

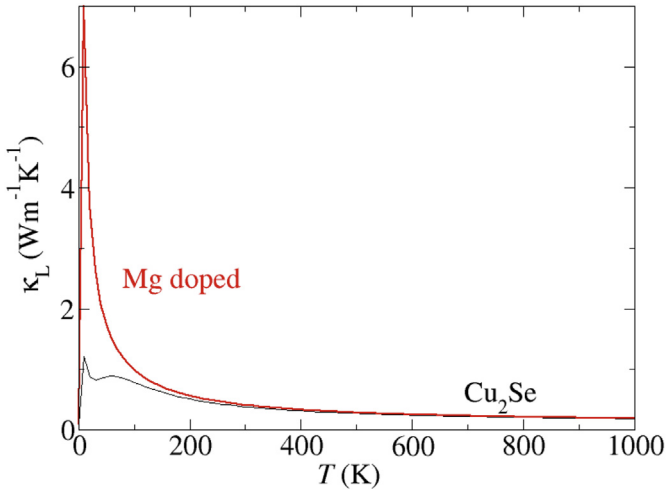

Fig. 7. The comparison of the calculated lattice thermal conductivity (κ_L) of pristine and 1.5 at. % Mg-doped Cu_2Se.

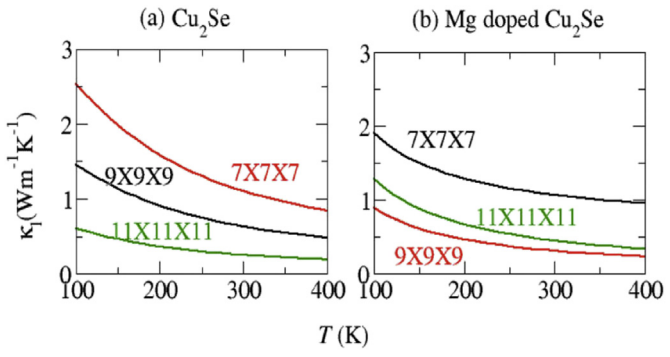

Fig. 8. The q mesh convergence of the lattice thermal conductivity (κ_L) of (a) pristine Cu_2Se and (b) Mg doped Cu_2Se plotted as a function of temperature T (K).

indicating *p*-type behaviour in all the samples. The β-phase of pristine and Mg-doped Cu_2Se shows a near-linear temperature dependence of the Seebeck coefficient, especially for the doped samples. The Seebeck coefficient of Mg-doped Cu_2Se is decreasing with increasing the doping concentration of Mg. A similar near-linear increase is observed in the temperature dependence of the electrical resistivity for β-phase of pristine and Mg-doped Cu_2Se samples (Fig. 5(b)), which suggests behaviour akin to degenerate semiconductors. Also, a general decrease in Seebeck coefficient is observed with increase in doping concentration of Mg, which may be attributed to the increase in carrier density with increasing Mg doping-concentration.

Fig. 5 (c), which shows the dependence in the electrical parameters of synthesized Cu_2Se as a function of the Mg doping (evaluated from the room temperature Hall measurements), suggests that although the carrier concentration increases with doping concentration, the mobility shows a corresponding decrease. This figure clearly explains the experimentally observed dependences of both the electrical conductivity as well as the Seebeck coefficient on the doping concentration. Although, in a manner similar to Na doped Cu_2Se [39], it is expected that donor doping of Mg in Cu_2Se should give more electrons and as a result the carrier concentration should decrease due to recombination of charge carriers. But in current study, the carrier concentration is increasing with increasing the Mg-doping content. This strange phenomenon may be ascribed to the concept of antidoping, which was also noticed in a number of cases [40]. Also, similar behaviour of carrier concentration has also been reported by Bailey et al. in Sn doped Cu_2Se [14].

Fig. 5 (d) shows the temperature dependence of the calculated power factor ($S^2\sigma$), which indicates that the power factor of Cu_2Se increases with Mg doping concentration, although in a non-monotonic fashion and a highest power factor $\sim 1.52 \times 10^3$ μW/mK^2 at 860 K has been realized for Cu_2Se doped with 1 at.% Mg, which is ~30% higher than its pristine counterpart and those reported earlier for Sn [14] and Te [16] doping in Cu_2Se. The main parameter responsible for this enhanced power factor is the increased electrical conductivity post Mg doping, which is attributed to the increment in the carrier concentration of the samples doped with Mg. Further, at elevated temperature the enhancement in electrical conductivity is even more prominent.

The plot of thermal conductivity with respect to temperature for the synthesized pristine as well as different Mg-doped Cu_2Se compositions is presented in Fig. 6(a), also the corresponding temperature dependent specific heat and thermal diffusivity are shown in the inset. The lattice thermal conductivity was calculated using the Wiedemann-Franz law ($\kappa_e = L\sigma T$), where L is the Lorentz number, which has been calculated from the temperature dependent Seebeck using equation $L = 1.5 + \exp[-|S|/116]$ (where L is in 10^{-8} WΩK^{-2} and S in μV/K) [41–43]. The lattice contribution was calculated by $\kappa = \kappa_e + \kappa_L$. the temperature dependent lattice and electronic thermal conductivity for synthesized pristine and different Mg-doped Cu_2Se samples is presented in Fig. 6(b), which suggest that the lattice thermal conductivity of the doped-Cu_2Se samples is found to be reasonably close to that of the pristine sample, regardless of the doping concentration, suggesting that the total thermal conductivity has a major contribution from its electronic counterpart. This has been substantiated by our theoretical calculation of the lattice thermal conductivity of Mg-doped and pristine Cu_2Se. We

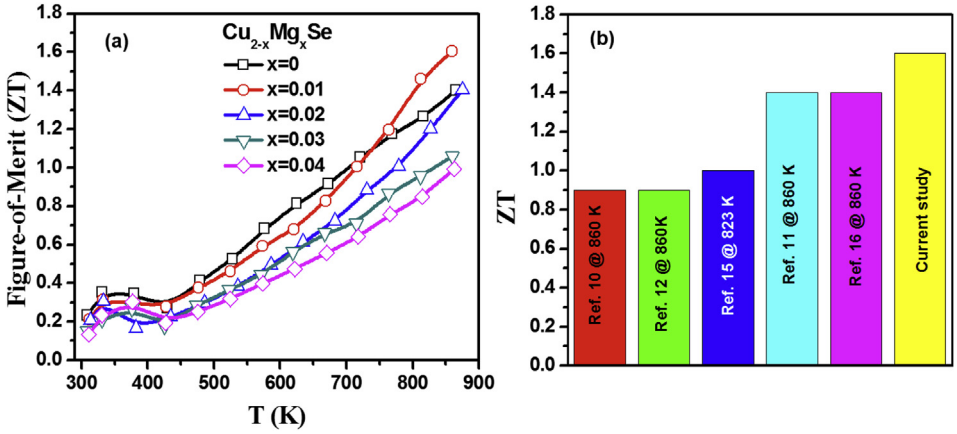

Fig. 9. (a) Temperature dependence of the figure-of-merit (ZT) of pristine and Mg-doped Cu_2Se and (b) A comparison of the reported ZT values of bulk Cu_2Se.

have explicitly checked the q-mesh convergence of κ_l, which is shown in Fig. 8. The lattice thermal conductivities are calculated from the third order force constants by using phono3py [36]. The force calculations are performed using the all electron full potential FHI-aims [44] code that uses numeric atom centered basis set. The phonon dispersion and the phonon density of states are calculated under the harmonic approximation using the finite displacement method as implemented in phonopy [35]. We have calculated the κ_l of the $2 \times 2 \times 2$ supercell of Cu_2Se, whereby we have explicitly checked its q-mesh convergence (cf. Fig. 8). The κ_l of Cu_2Se is calculated to be 0.38 $Wm^{-1}K^{-1}$ at 300 K. For the purpose of the calculation of the κ_l of the Mg doped case, we have substituted one Cu atom by Mg in the lattice of the $2 \times 2 \times 2$ Cu_2Se supercell with 64 Cu atoms. This leads to the case of 1.5% doping. The lattice thermal conductivity of Mg doped Cu_2Se, is found to be close to the lattice thermal conductivity of pristine β-Cu_2Se, which is reasonably close to its corresponding experimentally measured value (see Fig. 7). This endorses our prediction that the lattice thermal conductivity of Cu_2Se does not change significantly on doping, which can be attributed to the liquid like behaviour of Cu ions in Cu_2Se (as discussed in the references 9, 23, 24), which dominates the phonon scattering lifetimes and therefore, the lattice thermal conductivity.

Finally, the calculated temperature dependent figure-of-merit (ZT) for the pristine and Mg-doped compositions of Cu_2Se is shown in Fig. 9(a), which suggest a $(ZT)_{max} \sim 1.6$ at 860 K has been realized in the Cu_2Se doped with an optimized doping of 1 at.% Mg, which is the state-of-the-art value of ZT reported thus far in pristine or doped Cu_2Se [9,14,16,27], despite synthesized using a facile and fast process. A comparison of the reported values of ZT for pristine and doped Cu_2Se (in the temperature range of 800–860 K) has been shown in Fig. 9(b). Although much higher values of ZT have been earlier reported in doped Cu_2Se [11,12,14], but these were realized at much higher temperatures. However, we have confined our measurements to ~860 K in order to limit the Se-evaporation, which ensured reproducibility in our thermoelectric measurements. Although, recently R. Nunna et al. [45] and Olvera et al. [46] have reported a high $(ZT)_{max}$ in Cu_2Se/CNT hybrid nanocomposite and $Cu_2Se/CuInSe_2$ nanocomposites, respectively, but their synthesis involved multiple processing steps, which is both expensive and time-consuming. In comparison, we have achieved ZT ~1.6 at 860 K in bulk Cu_2Se doped with 1 at. % Mg employing a facile one-step reaction sintering route using spark plasma sintering, wherein the reaction and consolidation taken place in a single step and within a few minutes.

4. Conclusions

In summary, we have explored the possibility of enhancement of the thermoelectric performance of Cu_2Se by doping with Mg. Experimentally, an enhanced ZT ~1.6 at 860 K was realized in 1 at. % Mg-doped Cu_2Se, synthesized employing facile single-step reactive spark plasma sintering, which is both fast and scalable. While the experimentally determined electronic transport coefficients corresponding to Mg doping of Cu_2Se were found to enhance considerably over the pristine counterpart, the lattice thermal conductivity was found to be nearly-unaffected with doping concentration, which has also been confirmed by our DFT-based theoretical calculations. This may be attributed to the liquid-like behaviour of Cu ions in Cu_2Se that dominates the phonon scattering lifetimes to an extent that the doping induced changes in the lattice dynamics were found to be insignificant.

Declarations of interest

None.

Acknowledgments

The authors sincerely acknowledge the Board of Research in Nuclear Sciences, Department of Atomic Energy (Sanction No: 37(3)/14/22/2016-BRNS/37055), India for the financial support. Ruchi Bharadwaj would like to acknowledge the financial support from DST-India as INSPIRE-Junior Research Fellowship. The technical support rendered by Mr. Radhey Shyam, and Mr. Naval Kishor Upadhyay are also gratefully acknowledged. AB acknowledges the funding received from the DST Inspire faculty award grant (DST/INSPIRE/04/2015/000089) SA would like to acknowledge the use of the High Performance Computing (HPC) facilities at Physics Department of Indian Institute of Technology in Kanpur (IITK), Intra-University Accelerator Centre (IUAC) in New Delhi, Institute of Mathematical Sciences (IMSC)in Chennai, Council of Scientific and Industrial Research Fourth Paradigm Institute (CSIR-4PI) at Bangaluru and University of Hyderabad in Hyderabad.

References

[1] G.J. Snyder, E.S. Toberer, Complex thermoelectric materials, Nat. Mater. 7 (2008) 105–114.
[2] Y. Lan, A.J. Minnich, G. Chen, Z. Ren, Enhancement of thermoelectric figure-of-merit by a bulk nanostructuring approach, Adv. Funct. Mater. 20 (2010) 357–376.
[3] M. Zebarjadi, K. Esfarjani, M. Dresselhaus, Z. Ren, G. Chen, Perspectives on thermoelectrics: from fundamentals to device applications, Energy Environ. Sci. 5 (2012) 5147–5162.
[4] K. Tyagi, B. Gahtori, S. Bathula, V. Toutam, S. Sharma, N.K. Singh, A. Dhar, Thermoelectric and mechanical properties of spark plasma sintered Cu3SbSe3 and Cu3SbSe4: promising thermoelectric materials, Appl. Phys. Lett. 105 (2014) 261902.
[5] H. Wang, Y. Pei, A.D. LaLonde, G.J. Snyder, Heavily doped p-type PbSe with high thermoelectric performance: an alternative for PbTe, Adv. Mater. 23 (2011) 1366–1370.

[6] J.-i. Tani, H. Kido, Thermoelectric properties of Bi-doped Mg 2 Si semiconductors, Phys. B Condens. Matter 364 (2005) 218–224.
[7] N.K. Singh, S. Bathula, B. Gahtori, K. Tyagi, D. Haranath, A. Dhar, The effect of doping on thermoelectric performance of p-type SnSe: promising thermoelectric material, J. Alloy. Comp. 668 (2016) 152–158.
[8] X. Xing-Xing, X. Wen-Jie, T. Xin-Feng, Z. Qing-Jie, Phase transition and high temperature thermoelectric properties of copper selenide Cu2− xSe (0≤ x≤ 0.25), Chin. Phys. B 20 (2011) 087201.
[9] H. Liu, X. Shi, F. Xu, L. Zhang, W. Zhang, L. Chen, Q. Li, C. Uher, T. Day, G.J. Snyder, Copper ion liquid-like thermoelectrics, Nat. Mater. 11 (2012) 422.
[10] B. Yu, W. Liu, S. Chen, H. Wang, H. Wang, G. Chen, Z. Ren, Thermoelectric properties of copper selenide with ordered selenium layer and disordered copper layer, Nano Energy 1 (2012) 472–478.
[11] S. Ballikaya, H. Chi, J.R. Salvador, C. Uher, Thermoelectric properties of Ag-doped Cu 2 Se and Cu 2 Te, J. Mater. Chem. 1 (2013) 12478–12484.
[12] H. Liu, X. Yuan, P. Lu, X. Shi, F. Xu, Y. He, Y. Tang, S. Bai, W. Zhang, L. Chen, Ultrahigh thermoelectric performance by electron and phonon critical scattering in Cu2Se1-xIx, Adv. Mater. 25 (2013) 6607–6612.
[13] B. Gahtori, S. Bathula, K. Tyagi, M. Jayasimhadri, A. Srivastava, S. Singh, R. Budhani, A. Dhar, Giant enhancement in thermoelectric performance of copper selenide by incorporation of different nanoscale dimensional defect features, Nano Energy 13 (2015) 36–46.
[14] T.P. Bailey, S. Hui, H. Xie, A. Olvera, P.F. Poudeu, X. Tang, C. Uher, Enhanced ZT and attempts to chemically stabilize Cu 2 Se via Sn doping, J. Mater. Chem. 4 (2016) 17225–17235.
[15] X. Su, F. Fu, Y. Yan, G. Zheng, T. Liang, Q. Zhang, X. Cheng, D. Yang, H. Chi, X. Tang, Self-propagating high-temperature synthesis for compound thermoelectrics and new criterion for combustion processing, Nat. Commun. 5 (2014).
[16] S. Butt, W. Xu, M.U. Farooq, G.K. Ren, Q. Zhang, Y. Zhu, S.U. Khan, L. Liu, M. Yu, F. Mohmed, Enhanced thermoelectricity in high-temperature β-phase copper (I) selenides embedded with Cu2Te nanoclusters, ACS Appl. Mater. Interfaces 8 (2016) 15196–15204.
[17] Y. He, T. Day, T. Zhang, H. Liu, X. Shi, L. Chen, G.J. Snyder, High thermoelectric performance in non-toxic earth-abundant copper sulfide, Adv. Mater. 26 (2014) 3974–3978.
[18] W. Borchert, Gitterumwandlungen im system Cu2-xSe, Z. für Kristallogr. - Cryst. Mater. 106 (1954) 5–24.
[19] A. Stevels, F. Jellinek, Phase transitions in copper chalcogenides: I. The copper--selenium system, Recl. Trav. Chim. Pays-Bas 90 (1971) 273–283.
[20] R.M. Murray, R.D. Heyding, The copper–selenium system at temperatures to 850 K and pressures to 50 kbar, Can. J. Chem. 53 (1975) 878–887.
[21] Z. Vučić, O. Milat, V. Horvatić, Z. Ogorelec, Composition-induced phase-transition splitting in cuprous selenide, Phys. Rev. B 24 (1981) 5398.
[22] L. Gulay, M. Daszkiewicz, O. Strok, A. Pietraszko, Crystal structure of Cu2Se, Chem. Met. Alloys 4 (2011) 200–205.
[23] O. Milat, Z. Vučić, B. Ruščić, Superstructural ordering in low-temperature phase of superionic Cu2Se, Solid State Ionics 23 (1987) 37–47.
[24] L. Yang, Z.-G. Chen, G. Han, M. Hong, Y. Zou, J. Zou, High-performance thermoelectric Cu2Se nanoplates through nanostructure engineering, Nano Energy 16 (2015) 367–374.
[25] B. Zhong, Y. Zhang, W. Li, Z. Chen, J. Cui, W. Li, Y. Xie, Q. Hao, Q. He, High superionic conduction arising from aligned large lamellae and large figure of merit in bulk Cu1. 94Al0. 02Se, Appl. Phys. Lett. 105 (2014) 123902.
[26] G. Dennler, R. Chmielowski, S. Jacob, F. Capet, P. Roussel, S. Zastrow, K. Nielsch, I. Opahle, G.K. Madsen, Are binary copper sulfides/selenides really new and promising thermoelectric materials? Advanced Energy Materials 4 (2014).
[27] S.D. Kang, J.-H. Pöhls, U. Aydemir, P. Qiu, C.C. Stoumpos, R. Hanus, M.A. White, X. Shi, L. Chen, M.G. Kanatzidis, Enhanced stability and thermoelectric figure-of-merit in copper selenide by lithium doping, Materials Today Physics 1 (2017) 7–13.
[28] P. Qiu, M.T. Agne, Y. Liu, Y. Zhu, H. Chen, T. Mao, J. Yang, W. Zhang, S.M. Haile, W.G. Zeier, Suppression of atom motion and metal deposition in mixed ionic electronic conductors, Nat. Commun. 9 (2018) 2910.
[29] N.S. Chauhan, S. Bathula, A. Vishwakarma, R. Bhardwaj, B. Gahtori, A. Kumar, A. Dhar, Vanadium doping induced resonant energy levels for the enhancement of thermoelectric performance in Hf-free ZrNiSn half-heusler alloys, ACS Appl. Energy Mater. 1 (2) (2018) 757–764.
[30] P. Hohenberg, W. Kohn, Inhomogeneous electron gas, Phys. Rev. 136 (1964) B864–B871.
[31] W. Kohn, L.J. Sham, Self-consistent equations including exchange and correlation effects, Phys. Rev. 140 (1965) A1133–A1138.
[32] G. Kresse, G. Kresse, J. Hafner, Phys. Rev. B 49 (1994) 14251 Phys. Rev. B, 49 (1994) 14251.
[33] J.P. Perdew, K. Burke, M. Ernzerhof, Generalized gradient approximation made simple, Phys. Rev. Lett. 77 (1996) 3865–3868.
[34] R. Bhardwaj, A. Bhattacharya, K. Tyagi, B. Gahtori, N.S. Chauhan, S. Bathula, S. Auluck, A. Dhar, Tin Doped Cu3SbSe4: a Stable Thermoelectric Analogue for the Mid-temperature Applications, Materials Research Bulletin, 2019.
[35] A. Togo, F. Oba, I. Tanaka, First-principles calculations of the ferroelastic transition between rutile-type and CaCl 2-type SiO 2 at high pressures, Phys. Rev. B 78 (2008) 134106.
[36] A. Togo, L. Chaput, I. Tanaka, Distributions of phonon lifetimes in Brillouin zones, Phys. Rev. B 91 (2015) 094306.
[37] K. Tyagi, B. Gahtori, S. Bathula, S. Auluck, A. Dhar, Band structure and transport studies of copper selenide: an efficient thermoelectric material, Appl. Phys. Lett. 105 (2014) 173905.
[38] M. Råsander, L. Bergqvist, A. Delin, Density functional theory study of the electronic structure of fluorite Cu2Se, J. Phys. Condens. Matter 25 (2013) 125503.
[39] Z. Zhu, Y. Zhang, H. Song, X. Li, Enhancement of the thermoelectric properties of Cu 1.98 Se by Na doping, J. Electron. Mater. 47 (2018) 7514–7519.
[40] Q. Liu, G.M. Dalpian, A. Zunger, Antidoping in insulators and semiconductors having intermediate bands with trapped carriers, Phys. Rev. Lett. 122 (2019) 106403.
[41] H.-S. Kim, Z.M. Gibbs, Y. Tang, H. Wang, G.J. Snyder, Characterization of Lorenz number with Seebeck coefficient measurement, Apl. Mater. 3 (2015) 041506.
[42] A. Vishwakarma, S. Bathula, N.S. Chauhan, R. Bhardwaj, B. Gahtori, A.K. Srivastava, A. Dhar, Facile synthesis of nanostructured n-type SiGe alloys with enhanced thermoelectric performance using rapid solidification employing melt spinning followed by spark plasma sintering, Curr. Appl. Phys. 18 (2018) 1540–1545.
[43] R. Bhardwaj, B. Gahtori, K.K. Johari, S. Bathula, N.S. Chauhan, A. Vishwakarma, S.R. Dhakate, S. Auluck, A. Dhar, Collective effect of Fe and Se to improve the thermoelectric performance of unfilled p-type CoSb3 Skutterudites, ACS Appl. Energy Mater. 2 (2) (2019) 1067–1076.
[44] V. Blum, R. Gehrke, F. Hanke, P. Havu, V. Havu, X. Ren, K. Reuter, M. Scheffler, Ab initio molecular simulations with numeric atom-centered orbitals, Comput. Phys. Commun. 180 (2009) 2175–2196.
[45] R. Nunna, P. Qiu, M. Yin, H. Chen, R. Hanus, Q. Song, T. Zhang, M.-Y. Chou, M.T. Agne, J. He, Ultrahigh thermoelectric performance in Cu 2 Se-based hybrid materials with highly dispersed molecular CNTs, Energy Environ. Sci. 10 (2017) 1928–1935.
[46] A. Olvera, N. Moroz, P. Sahoo, P. Ren, T. Bailey, A. Page, C. Uher, P. Poudeu, Partial indium solubility induces chemical stability and colossal thermoelectric figure of merit in Cu 2 Se, Energy Environ. Sci. 10 (2017) 1668–1676.